Available online at www.sciencedirect.com
ScienceDirect
International Journal of Refractory Metals & Hard Materials 25 (2007) 310–317
International Journal of REFRACTORY METALS & HARD MATERIALS
www.elsevier.com/locate/ijrmhm

Control of eta carbide formation in tungsten carbide powders sputter-coated with (Fe/Ni/Cr)

C.M. Fernandes [a], A.M.R. Senos [a,*], M.T. Vieira [b]

[a] Department of Ceramics and Glass Engineering, CICECO, University of Aveiro, 3810-193 Aveiro, Portugal
[b] ICEMS – Mechanical Engineering Department, Polo 2 of University of Coimbra, 3030-201 Coimbra, Portugal

Received 29 May 2006; accepted 12 July 2006

Abstract

Composite powders of tungsten carbide with variable coating contents of Fe/Ni/Cr based alloys (1–15 wt.%) were prepared by sputtering. The coated powders have revealed a good performance to shape-forming and sintering. However, the presence of nanocrystalline coatings could enhance the formation of a brittle phase during sintering, named η-phase, $(M,W)_6C$. To investigate this effect, the powders were heat-treated at variable temperatures, up to 1400 °C. For comparison, conventionally prepared powders were studied, too, and the content of η-phase was found to be higher for the sputter-coated ones. This result is attributed to the content of binder elements with affinity to carbon, like chromium, enhanced by the difference on binder characteristics, such as nanocrystallinity and morphology. It was concluded that an effective control of the reaction can be achieved by increasing in the binder composition the ratio between the elements without affinity and those with affinity to carbon and/or enlarging the carbon content.

Keywords: Tungsten carbide; Coated powders; Fe/Ni/Cr; η-phase; M_6C

1. Introduction

The constant increase in the use of WC-based cemented carbides in new applications, where cobalt is not welcome, and the threat from the depleting resources of cobalt led to a great deal of research into the development of alternative cemented carbides compatible with the WC–Co based ones.

Early attempts have been made [1–9] to find a satisfactory alternative binder phase to cobalt in WC hard metals with similar mechanical properties. The efforts made in the replacement of cobalt by other transition metals of VIII group, as iron or nickel [7–12], revealed that it is possible to promote the densification of WC–(Fe/Ni) at temperatures near those used for WC–Co cemented carbides. However, it might be more difficult to obtain competitive mechanical properties and to find the optimum choice of carbon content for such alloys. The most suitable compositions, from a carbon control point of view, are those where neither η-phase $(M,W)_6C$ nor graphite are formed during the thermal cycle needed to sinter the material [13,14]. A vertical section of the phase diagram W–C–Fe, calculated to 10 wt.% Fe (Fig. 1a), shows that only very close compositions, between the points *a* and *b*, fulfill these conditions [15]. Moreover, in the present system, this range of compositions corresponds to carbon contents higher than the stoichiometric. The addition of Ni to the W–C–Fe system can enlarge the suitable composition range and move this region to more favourable carbon contents, closer to the stoichiometric, depending on the Ni:Fe ratio, as illustrated in Fig. 1b [12,16,17].

When the composition of Fe-rich binders is adjusted there are no occurrences of free carbon or of brittle η-phase in the WC composites and the mechanical properties, such as hardness, toughness and transverse rupture strength (TRS), indicate similar or even superior values to the WC–Co system [7–13]. The role of chromium in

* Corresponding author. Tel.: +351 234 370257; fax: +351 234 425300.
E-mail address: anamor@cv.ua.pt (A.M.R. Senos).

0263-4368/$ - see front matter © 2006 Elsevier Ltd. All rights reserved.
doi:10.1016/j.ijrmhm.2006.07.004

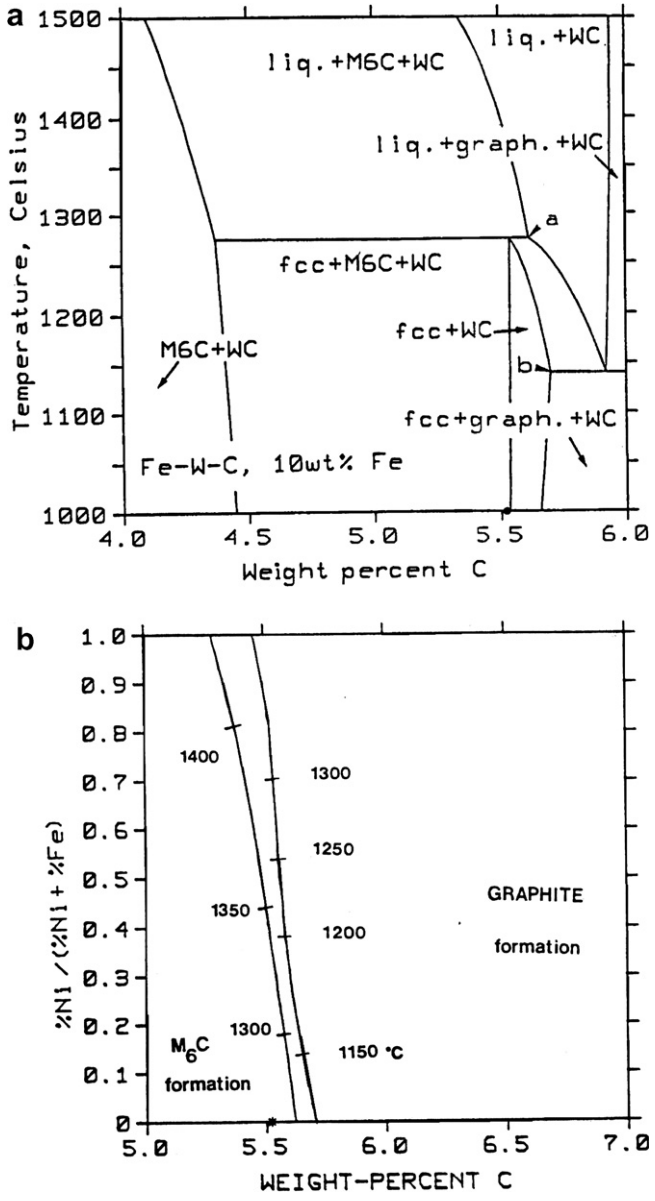

Fig. 1. (a) Vertical section of the Fe–W–C phase diagram, calculated at 10 wt.% Fe (from Ref. [15]). (b) Temperature projection of a section of the Fe–Ni–W–C phase diagram calculated at Fe + Ni = 10 wt.%. The lines describe the compositions of a mixture of WC and liquid in equilibrium with fcc + M_6C (to the left), and of a mixture of WC + fcc in equilibrium with liquid + graphite (to the right) (from Ref. [16]). The solid symbol on the composition axis on both pictures indicates the stoichiometric composition.

the binder has also been investigated, because it acts as a strong grain growth inhibitor and improves oxidation and corrosion resistance [13]. However, the presence of this element, which has more affinity to the carbon than the iron, obliges to an increase of the carbon content to avoid the formation of η-phase [12].

In the authors' own studies [18–21], tungsten carbide powders were sputter-deposited with stainless steel 304 AISI (71%Fe, 8%Ni, 18%Cr, 2%Mn and 0.07%C) by an innovative technique to produce composite powders. The aim of the selection of this binder is to induce two roles: (i) to improve the quality of the powder surfaces and (ii) to establish the optimum composition for the different elements studied. The structure, morphology and chemical distribution of the coated powders have already been investigated [18,19] and revealed that all the WC particles were uniformly coated and show "rough" surfaces, coming from the columnar growth of the thin film deposited [18,19]. The coated powder presents a WC major crystalline phase, traces of W_2C coming from the bulk, and a ferrite b.c.c. structure (Fe-α) for the sputtered layer.

The processing of these coated powders does not need a pressing binder, commonly used in the WC based cemented carbide powders. Sintering performed in a vacuum atmosphere provides high relative densities, ~96%, at a relatively low temperature of 1325 °C for compacts with an initial content of 10 wt.% of stainless steel [20,21]. This is a consequence of the low *liquidus* temperature, $T \simeq$ 1150 °C, and good wettability of the liquid phase to the powders to be sintered, together with the nanometer character and the highly uniform distribution of the coating induced by the sputtering process [18–21]. However, these qualities can enhance the formation of η-phase during the deposition process and sintering.

In this work, an attempt has been made to study η-phase formation with respect to the heating temperature, holding time, binder composition, namely the Ni/(Fe + Cr) ratio, and the carbon content. The optimization of the best ratio between elements with affinity and no-affinity to carbon was envisaged. The conclusions might be applied to coated and uncoated powders.

2. Experimental

WC powder particles were coated with stainless steel by d.c. magnetron sputtering. The deposition chamber was tailored to powder coating by a rotation and vibration of the substrate holder [18].

The powder is a fully carburized WC (9–10 μm) (H.C. Starck, HCST-Germany), which contains, besides the WC phase, traces of W_2C phase. The coatings were sputter-deposited on the WC particles from a target, consisting of a commercial type AISI 304 stainless steel disc (71%Fe, 8%Ni, 18%Cr, 2%Mn and 0.07%C). To increase the Ni/Fe ratio, high purity nickel discs have been bonded to the target. The percentage and the chemical composition of the binder phase in the coated powders (C–WC1 to C–WC6) were characterized by inductively coupled plasma–atomic emission spectrometry (ICP, Isa JY70Plus) in Table 1.

Conventional mixtures have also been prepared with uncoated WC powder and an admixed binder (Fe/Cr18/Ni10 Goodfellow FE226010 powder alloy), with a chemical composition similar to that of the coating of coated powders. Other binder compositions have been also prepared using different contents of iron (Goodfellow FE006020), chromium (Goodfellow CR006021/22) and nickel (Goodfellow NI006021/11) powders (Tables 2 and 3).

Table 1
Chemical compositions given by ICP of the sputter-deposited coatings on WC powders

Sample	wt.% Fe	wt.% Cr	wt.% Ni	wt.% Mn	$\frac{Ni}{Fe+Cr}$	Sum (wt.%)
WC[a]	0.02	<0.009	<0.009	<0.009	–	0.0
C–WC1	0.68	0.18	0.07	0.01	0.1	0.9
C–WC2	3.13	0.81	0.35	0.06	0.1	4.4
C–WC3	4.01	1.06	0.48	0.10	0.1	5.7
C–WC4	7.16	1.87	0.81	0.14	0.1	10.0
C–WC5	10.80	2.92	1.30	0.25	0.1	15.3
C–WC6	2.57	0.65	3.66	0.05	1.1	6.9

[a] Non-coated WC powder, presented for comparison.

The proportionated powders were milled with 1.5 wt.% of paraffin wax, using isopropyl alcohol as solvent, in a stainless steel mill with WC–Co balls, for 6 h. The mixture was subsequently dried at 60 °C, granulated and sieved. Graphite powder (Panreac 1221) with a maximum particle size of 20 μm has been added to the conventional and coated mixtures, in a dry mixer, for 1 h.

Pellets with 10 mm in diameter and about 3 mm thick were prepared by uniaxial pressing, at 190 MPa. The compacts from coated and conventional mixtures were heated in a vacuum furnace inside of a graphite crucible. The furnace atmosphere was pumped to a vacuum of 10 Pa before heating. The heating cycle involved a constant heating rate of 5 °C min^{-1} up to the maximum temperature, a holding time from 1 to 3 h and a cooling rate of 5 °C min^{-1} until ~800 °C, followed by the natural cooling rate of the furnace to room temperature.

The microstructural characterization was done by scanning electron microscopy (SEM, Hitachi-S4100) with energy dispersive spectroscopy (EDS, detector Rontec-EDR288/SPU2) on polished surfaces. An electron microprobe (EMPA-SX50, Cameca) was also used for chemical phase analysis.

The structural characterization of the as-coated and uncoated powders and heat-treated samples was performed by X-ray diffraction (XRD, Rigaku PMG-VH), after desegregation of the heat-treated compacts, using a CuK_α radiation ($\lambda = 1.5418$ Å).

The phase quantification was derived from Rietveld analyses of XRD spectra with the aid of the GSAS suite [22]. To achieve better results, each sample was analysed three times and the quantification of WC and η-phase was performed with the structure parameters available in the bibliography for the hexagonal WC crystalline phase [23] and the cubic η-phase Fe_3W_3C [24]. The modifications on the structure parameters, coming from the substitution of some Fe for Ni and Cr in the eta-carbide phase, η-phase, were neglected, as well as the interference of the Fe-α and Fe-γ phases with the quantification. The equivalent amounts of WC and η-phases achieved by stereology, using an areas ratio, on a polished surface of a C–WC3 sample heat-treated at 1200 °C, are indicative that these assumptions are acceptable in the present Rietveld determinations. On the other hand, the quantification of the Fe-α and Fe-γ crystalline phases in the coated powders were not successful due to a significantly enlarged peak area, caused by the nanometer grain size of the sputtered powders and residual stresses. Moreover, the diminishing quantity of those phases reduces the diffraction spectra to only one quantifiable peak, (1 1 0) Miller index for Fe-α and (1 1 1) for Fe-γ.

Table 2
Characteristics of the starting powders used in conventional mixtures, as given by suppliers

Powder	Maximum particle size (μm)	Purity/composition (wt.%)
Stainless steel AISI 304	45	/Fe 72; Cr 18; Ni 10
Iron	60	99/
Chromium	38	99/
Nickel	7	99/

Table 3
Chemical formulation of the conventional mixtures

Sample	wt.% Fe	wt.% Cr	wt.% Ni	$\frac{Ni}{Fe+Cr}$	Sum (wt.%)
M–WC1	2.9	0.7	0.4	0.1	4.0
M–WC2	4.6	1.2	0.7	0.1	6.5
M–WC3	7.2	1.8	1.0	0.1	10.0
M–WC4	10.8	2.7	1.5	0.1	15.0
M–WC5	5.8	1.4	2.8	0.4	10.0
M–WC6	3.6	0.9	5.5	1.2	10.0

3. Results and discussion

3.1. Structural evolution during heating

The sputtered powders have different amounts of coating, variable between ~1 and 15 wt.% (C–WC1 to C–WC5, in Table 1). The coated powder C–WC6 has a different binder composition with a higher Ni/(Fe + Cr) ratio, when compared with that of the other coated powders.

As-deposited coated powders do not reveal by X-ray diffraction the presence of η-phase. In order to evaluate the formation of phases during heating, the C–WC3 powder with 5.7 wt.% of binder (Table 1) was heated to different temperatures and the crystallographic phases were analysed by XRD. As reported in Fig. 2, the XRD diffraction profiles show the presence of the WC as major phase and another secondary phase, identified as η-phase $(M,W)_6C$, in all the studied temperatures above 750 °C. Moreover, a ferrite phase (Fe-α) was detected in the as-coated powder, becoming vestigial for temperatures higher than 800 °C. The reduction of the ferrite phase content was caused by its reaction with the WC grains to form $(M,W)_6C$ and, additionally, by the transition for an austenitic form, Fe-γ, more stable at high temperatures, Fig. 2.

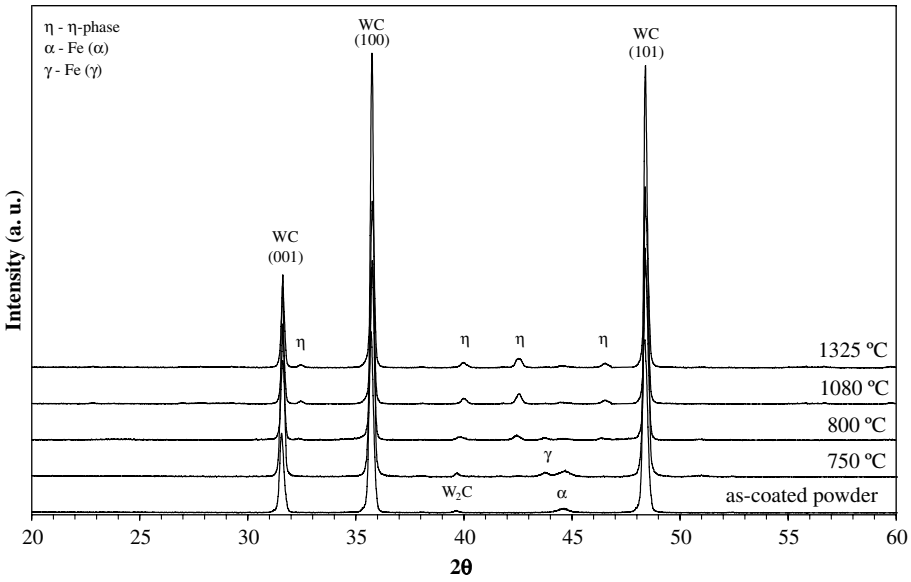

Fig. 2. XRD diffraction profiles of C–WC3 samples heated at different temperatures, for 3 h.

The $(M,W)_6C$ is the stable phase, like in W–C–Fe systems [17,25].

The microstructure of a polished C–WC3 surface, sintered for 3 h at 1200 °C, in Fig. 3, shows near dense WC grains and an intergranular phase, darker than the matrix. The points identified in Fig. 3 with α, β, χ, indicate the places were EMPA analyse have been performed. The analysis in point α, inside a WC grain, presents an excess of carbon, caused by the impregnation with resin, needed for the sample polishing. The detection of other elements, besides W and C, in the analysis of point α has been related to the width of the electronic beam, catching the interference of other phases, namely the η-phase, since the solubility of Fe, Ni and Cr in WC is very low [12,26]. The EMPA analysis at the points β and χ, inside the darker phase, shows that this phase is richer in Fe, Cr and Ni, and also contains an appreciable amount of W, as expected for the $(M,W)_6C$ phase. Taking the EMPA analysis done in several points (five determinations), the stoichiometry of this phase is $(Fe_{2.3}Ni_{0.3})(Cr_{0.6}W_{2.8})C$. This composition of the $(M,W)_6C$ phase remains constant, within the experimental error, with the increase in temperature from 1200 to 1325 °C, or with the increase of the binder amount (5.7–10 wt.%) in the WC-stainless steel AISI 304 composites. The main binder elements, Fe, Ni and Cr, are systematically detected in the $(M,W)_6C$ phase within atomic proportions close to that found in the binder (see table inserted in Fig. 3). The easy accommodation of metal elements (Ti, V, Ta, Cr, Mo) in the M_6C structure was already observed in the WC–Co system, where both W and Co could be partially substituted by other metal additives [27,28].

3.2. Eta carbide formation: effect of temperature, time and binder amount

The percentage of η-phase, relative to the total amount of the main crystalline phases, η and WC, calculated from the XRD data, vs. the heating temperature, for a holding time of 3 h, is shown in Fig. 4 for the C–WC3 powder. The figure shows that the η-phase formation starts at low temperatures, near 750 °C, and its amount gradually

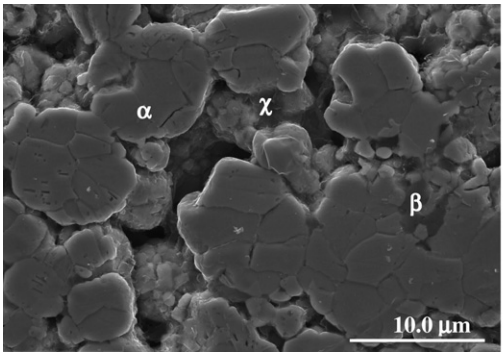

EMPA Analysis (Atomic percentages)

Point	W	Fe	Cr	Ni	C
α	32.1	4.4	0.8	0.4	62.3
β	23.3	24.2	5.0	2.3	45.2
χ	23.8	26.3	5.7	2.0	42.2

Fig. 3. SEM micrograph and EMPA analysis of a C–WC3 (5.7%) compact heat-treated at 1200 °C, for 3 h.

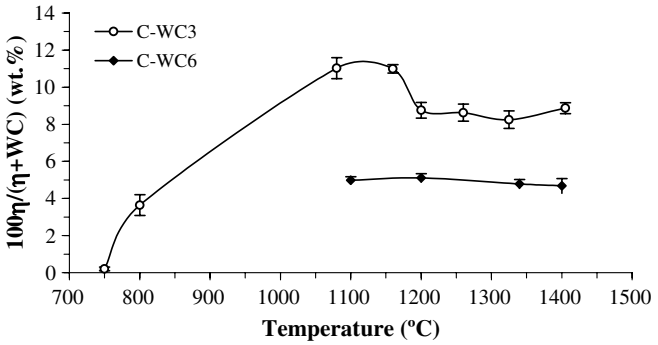

Fig. 4. Amount of M_6C phase vs. heating temperature (holding time of 3 h) for C–WC3 and C–WC6 samples.

increases until ~1100 °C. The densification results of this composite powder indicate that the liquid phase appears only at temperatures ~1150 °C [20]. So, the $(M,W)_6C$ phase is formed by a solid state reaction at temperatures significantly lower than those of the liquid phase formation. When the liquid phase forms, ~1150 °C, some dissolution of the η-phase is observed to occur in Fig. 4. It must also be pointed that as a consequence of the high content of η-phase formed at low temperatures in these systems, the amount of binder elements available for the liquid phase formation, at higher temperatures, is significantly reduced.

The variation of the relative amount of $(M,W)_6C$ phase with the initial binder content is shown in Fig. 5, for powders with a constant binder composition (C–WC1 to C–WC5 powders, Table 1) heated at 1325 °C, for 3 h. A near-linear relation with a positive slope of ~1.7 was found. This relation means that increasing the binder content both increases the amount of η-phase and the amount of binder elements available to form a liquid phase.

Also represented in Fig. 5 are data for conventionally prepared composites powders with compositions equivalent to those of the coated powders and using the same heating schedule. It can be observed that a near-linear relation between the η-phase percentage and the binder amount was also obtained but, in this case, the slope is smaller, ~0.8. So, comparing the results of coated and conventionally prepared powders, it is verified that in the coated powders the formation of η-phase is much more extended, being formed in the double amount than in admixed powders with the same composition. The differences between coated and conventionally prepared powders are related to the much higher uniformity of the binder distribution attained in the sputtered powders, together with the nanometer particle size in the sputtered coating. In consequence, a larger increase of the contact area between the WC and the binder phases with a strong decrease of the diffusion distances needed to transport the species for $(M,W)_6C$ formation would be expected. If this is the case, the formation of this phase must be controlled by the species diffusion, after an initial fast nucleation step.

The kinetic of the $(M,W)_6C$ phase formation was studied at 800 °C, both in sputtered and conventional prepared powders with 10 wt.% of binder (Fig. 6). It can be observed in Fig. 6a that, as expected, an equivalent amount of $(M,W)_6C$ is rapidly formed in both powders, within the first 5 min. After, the rate of formation is reduced and this reduction is more pronounced for the conventional mixture. The representation of Avrami for these data is presented in Fig. 6b. A slope of $n = 0.6$ was determined for the coated powder, identified by the Avrami law with a

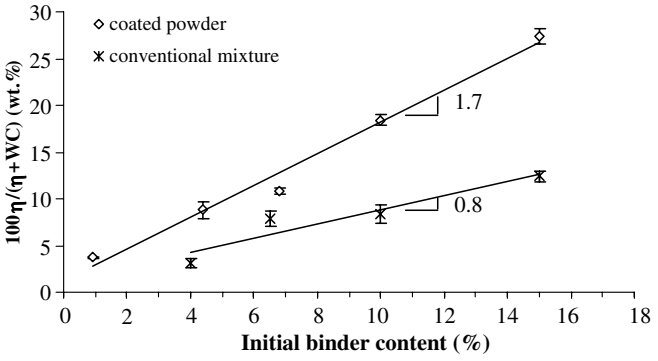

Fig. 5. Amount of M_6C phase vs. initial binder content for coated and admixed powder compacts heated at 1325 °C (3 h hold time).

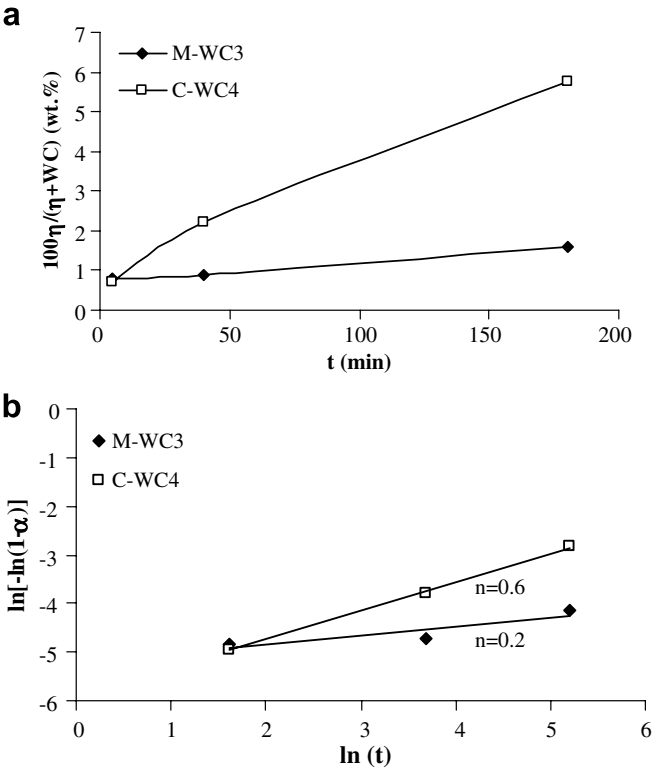

Fig. 6. Relative amount of M_6C vs. time at 800 °C for M–WC3 and C–WC4 powder compacts: (a) linear representation; (b) Avrami representation.

growth process of the η-phase effectively controlled by diffusion. The slope found for the conventionally prepared powder, $n = 0.2$, is lower than the theoretical range of predicted values, but a diffusion controlled mechanism is yet the most probable.

3.3. Control of eta carbide formation

The occurrence of η-phase is related to a carbon deficit, caused by decarburisation during sintering, or to a carbon content in the initial composition below the necessary to prevent the formation of η-phase. This phase being formed at relatively low temperatures, before the formation of any liquid phase, decarburisation is not expected to be significant. Other relevant phase diagrams, namely for the W–C–Fe [15,29] and for W–C–Fe–Ni [16,17] systems, show that the carbon content needed to avoid the precipitation of η-phase could be higher than the stoichiometric one (as shown in Fig. 1). The effect of Cr on the favourable carbon content is not established but it is known that Cr is a carbide former [11,13,30], suggesting that the carbon content must be increased further to avoid η-phase formation. Therefore, in a WC–Fe–Cr–Ni system with a low Ni/(Fe + Cr) ratio and a stoichiometric carbon content the formation of η-phase would be unavoidable. These conditions are met in the present system, with an AISI 304 stainless steel binder (~72 wt.% Fe, ~18 wt.% Cr, ~10 wt.% Ni as the main elements) and a near stoichiometric WC powder (actually, a slight carbon deficiency of ~0.3 wt.% was experimentally determined).

The formation of the η-phase being thermodynamically favoured in these compositions and kinetically accelerated by the morphology and the nanocrystallinity in the sputtered coated powders, significant amounts may be formed, as shown in Figs. 4 and 5. One approach to reduce the amount of η-phase is the adjustment of the binder composition in order to move the limits of the two-phase region to lower carbon contents. As previously noted, the enrichment of the binder composition with Ni could have the desired effect and this was first tested in conventional mixtures (M–WC), where it is easier to control both the composition and the content of binder. The impact of the Ni/(Fe + Cr) ratio between 0.1 (for AISI 304 stainless steel) and 1.2 in powders with 10 wt.% binder, sintered at 1100 °C, is shown in Fig. 7. The percentage of η-phase was effectively reduced from ~12 wt.% to ~4 wt.%. For coated powders (C–WC) with 6–7 wt.% binder, the increase of the Ni content from 0.1 to 1.1 also brought an equivalent reduction of the η-phase from ~11 wt.% to ~4.5 wt.% (see Fig. 7). This amount of $(M,W)_6C$ does not significantly change within the sintering temperature range, 1100–1400 °C, as is shown in Fig. 4.

Although an effective reduction of the η-phase was achieved by the Ni enrichment of the initial binder composition, the elimination of that phase will require yet a larger Ni content. For the conventional prepared powders with 10 wt.% binder, this content can be estimated to

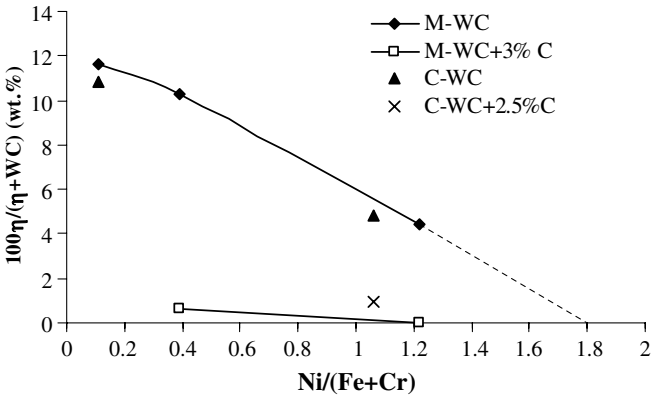

Fig. 7. Binder composition vs. relative amount of M_6C formed at 1100 °C, 1 h, in admixed powders (M–WC) with 10 wt.% of binder and in coated powders (C–WC) with 6–7 wt.% of binder.

Ni/(Fe + Cr) ratio ≈1.8 (Fig. 7) and even larger amounts would be needed for equivalent binder amounts in the sputter-coated powders. Such an increase of the Ni content would also increase the sintering temperatures [13,26]. As a consequence, during conventional sintering, densification and weight losses are difficult to control, as experimentally tested by our team, and production costs increase. In this sense, an adjustment of the carbon content in powders has been tried as a complementary way to further reduce the η-phase amount.

Carbon additions were performed in conventionally admixed as well as in coated powders. For the conventional powders, M–WC5 and M–WC6, with 10 wt.% of binder, 3 wt.% carbon in excess, relative to the stoichiometric carbon, were added, and for the coated powder, C–WC6, with 6 wt.% of binder, an excess of 2.5 wt.% was applied. The XRD profiles for M–WC6 and C–WC6 powders heated at 1100 °C, 1 h, are presented in Fig. 8. For the C–WC6 powder the M_6C phase became residual. For the M–WC6 powder, only the WC phase and Fe-γ phases are observed. No graphite phase was detected in any case. The corresponding amount of η-phase, calculated from the XRD data, are also represented in Fig. 7, confirming that none or very low amounts of η-phase are formed in these powders with a higher Ni content and excess carbon. So, by an adequate Ni enrichment of the binder composition and the use of excess carbon, it is possible to dramatically reduce, or even eliminate, the $(M,W)_6C$ formation in W–C–Fe–Ni–Cr system. The reactivity control during the heat-treatment necessary to obtain dense samples provided us the technological basis to obtain sintered compacts with similar compositions, but different structural characteristics. In a continuation of this work, the mechanical behaviour of such composites, obtained from sputtered-coated powders is currently under study. Actually, one of the aspects investigated is the effect of the η-phase content, since the higher dispersion of this phase attained in the coated powder samples, compared to conventional powders,

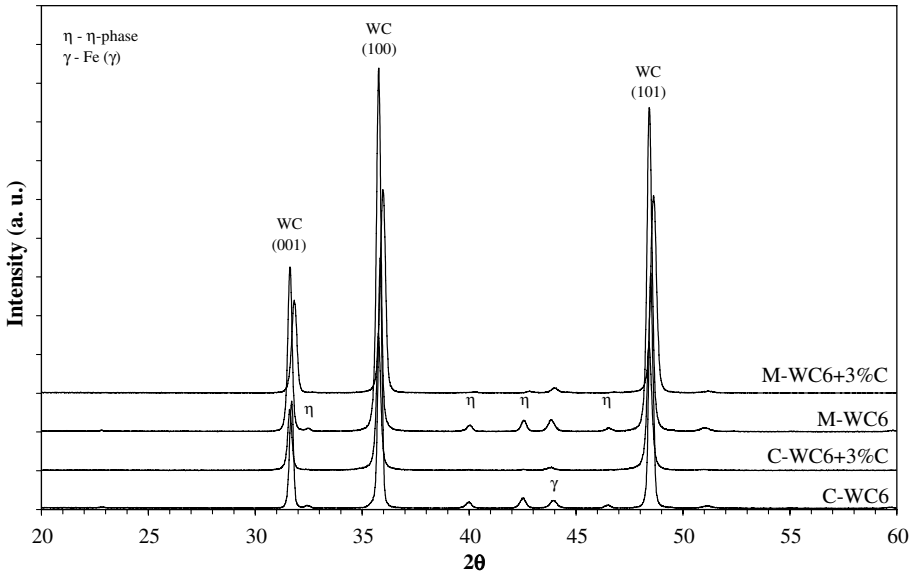

Fig. 8. XRD diffraction profiles of C–WC6 and M–WC6 powders, with and without carbon addition, heated at 1100 °C, for 1 h.

can minimize its deleterious role in the mechanical properties.

4. Conclusions

The formation of η-phase in composite powders of WC sputter-coated with stainless steel AISI 304 starts at about 750 °C, increases up to 1100 °C, and continues until the maximum studied temperature, 1400 °C. The η-phase, in the temperature range 1200–1325 °C, can be represented approximately as $(Fe_{2.3}Ni_{0.3})(Cr_{0.6}W_{2.8})C$ ($(M,W)_6C$). The main binder elements (Fe, Ni, Cr) are easily accommodated in the $(M,W)_6C$ structure.

The amount of η-phase is higher in coated than in the admixed powders with similar chemical composition and the same processing conditions. The $(M,W)_6C$ phase is formed by a solid state reaction with the growth process controlled by diffusion. The much higher uniformity of the binder distribution and the nanometric character of the thin film in the sputtered powders lead to an increase in contact area between the WC and the binder phases, and to a decrease of diffusion distances, compared with traditional micrometrics binders.

In both cases the amount of η-phase is reduced by increasing the Ni/(Fe + Cr) ratio from 0.1 to 1.1. Additionally, 2.5–3 wt.% excess carbon can eliminate the $(M,W)_6C$ phase. Thus, by a suitable elemental variation it is possible to control the reaction between the WC particles and the Fe/Ni/Cr binder during the heating process, which is crucial to control selected structural properties.

Acknowledgements

The authors wish to thank Dr. Maxim Avdeev and Dr. Dimitry Khalyavin for the help in the analysis of XRD data. The author C.M. Fernandes gratefully acknowledges the financial support of the POCTI programme of the Portuguese Foundation for Science and Technology (FCT) and European Social Fund (FSE).

References

[1] Suzuki H, Yamamoo T, Kawakatsu I. Properties of WC–10%(Ni–Fe). Powder Metall J 1967;14:26–31.
[2] Moskowitz D, Ford MJ, Humenik Jr M. High-strength tungsten carbides. Int J Powder Metall 1970;6(4):55–64.
[3] Moskowitz D. Abrasion resistant iron–nickel bonded tungsten carbide. Mod Dev Powder Metall 1977;10:543–51.
[4] Moskowitz D, Ford MJ, Humenik Jr M. High-strength tungsten carbides. Mod Dev Powder Metall 1971;5:225–34.
[5] Miodownik AP. Means of predicting structure and performance of new materials. Powder Metall 1989;32(4):269–76.
[6] Farroq T, Davies TJ. Tungsten carbide hard metals cemented with ferroalloys. Int J Powder Metall 1991;27(4):347–55.
[7] Viswanadham RK, Lindquist PG. Transformation-toughening in cemented carbides: Part I. Binder composition control. Metall Trans A 1987;18A:2163–73.
[8] Kakeshita T, Wayman CM. Martensitic transformations in cements with a metastable austenitic binder. Mater Sci Eng 1991;A141:209–19.
[9] Uhrenius B. Phase diagrams as a tool for production and development of cemented carbides and steels. Powder Metall 1992;35(3):203–10.
[10] González R, Echeberría J, Sánchez JM, Castro F. WC-(Fe, Ni, C) hardmetals with improved toughness through isothermal heat treatments. J Mater Sci 1995;30(13):3435–9.
[11] Cooper R, Manktelow SA, Wong F, Collins LE. The sintering characteristics and properties of hard metal with Ni–Cr binders. Mater Sci Eng A 1988;A105–106:269–73.
[12] Tracey VA. Nickel in hardmetals. Int J Refr Metals Hard Mater 1992;11:137–49.
[13] Penrice TW. Alternative binders for hard metals. Carbide Tool J 1988;20(4):12–5.
[14] Uhrenius B. On the composition of Fe–Ni–Co–WC-based cemented carbides. Int J Refr Metals Hard Mater 1997;15:139–49.
[15] Guillermet AF. The Co–Fe–Ni–W–C phase diagram: a thermodynamic description and calculated sections for (Co–Fe–Ni) bonded cemented WC tools. Metallkd 1989;80(2):83–94.

[16] Guillermet AF. An assessment of the Fe–Ni–W–C phase diagram. Metallkd 1987;78(3):165–71.
[17] Guillermet AF. Use of phase-diagram calculations in selecting the composition of Fe–Ni bonded WC tools. Int J Refr Metals Hard Mater 1987;6(1):24–7.
[18] Fernandes CM, Ferreira VM, Senos AMR, Vieira MT. Stainless steel coatings sputter-deposited on tungsten carbide powder particles. Surf Coat Technol 2003;176(1):103–8.
[19] Fernandes CM, Senos AMR, Vieira MT. Particle surface properties of stainless steel-coated tungsten carbide powders. Powder Technol 2006;164(3):124–9.
[20] Fernandes CM, Senos AMR, Vieira MT. Sintering of tungsten carbide particles sputter-deposited with stainless steel. Int J Refr Metals Hard Mater 2003;21:147–54.
[21] Fernandes CM, Senos AMR, Vieira MT. Study of sintering variables of tungsten carbide particles sputter-deposited with stainless steel. Mater Sci Forum 2004;455–456:295–8.
[22] Larson AC, Von Dreele RB. LAUR 86-748 Report, General structure analysis system. Los Alamos National Laboratory, 1990.
[23] Leiciejewicz J. A note on the structure of tungsten carbide. Acta Cryst 1961;14:200.
[24] Yang Q, Andersson S. Application of coincidence site lattices for crystal structure description. Part I: $\Sigma = 3$. Acta Cryst 1987;B43:1–14.
[25] Åkesson L. Thermodynamic and sintering studies in the Co–W–C system. Thermochim Acta 1979;29:327–32.
[26] Upadhyaya GS, Bhaumik SK. Sintering of submicron WC–10 wt.% Co hard metals containing nickel and iron. Mater Sci Eng A 1988;A105–106:249–56.
[27] Åkesson L. An experimental and thermodynamic study of the Co–W–C system in the temperature range 1470–1700 K. In: Viswanadham RK, Rowcliffe DJ, Gurland J, editors. Science of hard materials. New York: Plenum Press; 1983. p. 71–82.
[28] Pollock CB, Stadelmaier HH. The eta carbides in the Fe–W–C and Co–W–C systems. Metall Trans 1970;1:767–70.
[29] Bergström M. The eta carbides in the ternary system Fe–W–C at 1250 °C. Mater Sci Eng 1977;27:257–69.
[30] Bergström M. The eta carbides in the quaternary system Fe–W–C–Cr at 1250 °C. Mater Sci Eng 1977;27:271–86.